Thickness effects on the magnetism of Ho thin films



2005 J. Phys.: Condens. Matter 17 2543

(http://iopscience.iop.org/0953-8984/17/17/002)

INSTITUTE OF PHYSICS PUBLISHING JOURNAL OF PHYSICS: CONDENSED MATTER

J. Phys.: Condens. Matter **17** (2005) 2543–2552 doi:10.1088/0953-8984/17/17/002

# Thickness effects on the magnetism of Ho thin films

**A D F Herring[1,6], W J Nuttall[2], M F Thomas[1], J P Goff[1], A Stunault[3], R C C Ward[4], M R Wells[4] and W G Stirling[1,5]**

[1] Department of Physics, University of Liverpool, Oxford Street, Liverpool L69 7ZE, UK
[2] Judge Institute of Management (and Cambridge University Engineering Department), Trumpington Street, Cambridge CB2 1AG, UK
[3] Institut Laue-Langevin, 6 rue Jules Horowitz, BP156, F-38043 Grenoble Cedex 09, France
[4] Department of Physics, Clarendon Laboratory, Oxford University, Parks Road, Oxford OX1 3PU, UK
[5] European Synchrotron Radiation Facility, BP220, F-38043 Grenoble Cedex 09, France

E-mail: adfh@cmp.liv.ac.uk

Received 6 August 2004, in final form 24 March 2005
Published 15 April 2005
Online at stacks.iop.org/JPhysCM/17/2543

**Abstract**

This study was undertaken to probe any thickness dependence of the magnetic ordering in Ho film samples of thickness 1000 monolayers (ML), 100 ML and 50 ML. The study was carried out on the antiferromagnetic helical magnetic phase in the temperature range 65 $\rightarrow$ 132 K ($T_N$). The magnetism was studied by x-ray magnetic scattering using the resonant process at the Ho $L_{III}$ absorption edge, 8.071 keV. It was found that the magnetic modulation wavevector, $\tau$, of the Ho helical structure changed systematically with temperature over the range 65 K $\rightarrow$ $T_N$. No evidence of a change in $\tau$ with changing layer thickness was seen. The value of the Néel temperature $T_N$ decreased from 130 K for the 1000 ML sample to 110 K for the 50 ML sample. The critical exponent $\beta$ of the transition between the helical to paramagnetic state is measured as $\beta \approx 0.5$ for the 1000 and 100 ML samples compared to a literature value of $\beta = 0.39$ for bulk. For the 50 ML film, $\beta = 0.28 \pm 0.05$. The measured values of $\beta$ are discussed in terms of strain and reduced dimensionality.

## 1. Introduction

Metallic holmium crystallizes in an hcp structure with room temperature lattice parameters $a = 3.58$ Å and $c = 5.616$ Å [1]. The magnetic structure of holmium below the ordering temperature of 132 K consists of ferromagnetic sheets with moments confined to the basal $a$–$b$ plane but with a rotation of the ferromagnetic axis from plane to plane up the $c$ axis to form a helical structure. This structure, determined by neutron diffraction [2–5], and further studied by magnetic x-ray diffraction, persists with decreasing temperature to a value of 20 K,

[6] Author to whom any correspondence should be addressed.

  

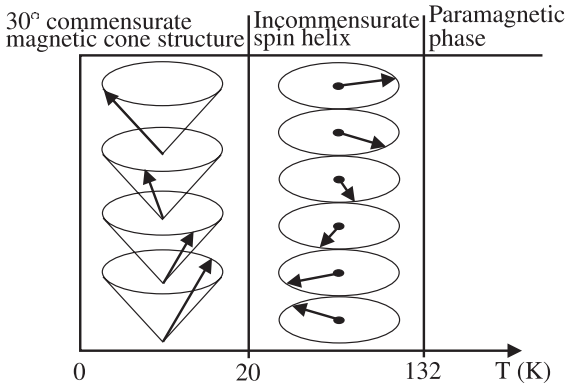


**Figure 1.** Magnetic phase diagram of bulk holmium illustrating the alignment of the magnetic moments within the hexagonal layer planes.

where a transition occurs to a structure showing a helical evolution in the *a–b* planes but with a ferromagnetic component along the *c* axis. The structures are illustrated schematically in figure 1.

There is presently much interest in the study of magnetic samples composed of thin films of magnetic and non-magnetic metals. In the study of such multilayer samples the question arises whether the magnetic properties of a magnetic layer are affected by the layer thickness. Factors that may modify the magnetic behaviour in layers in the few monolayers thickness range are the reduced dimensionality of the magnetic interactions and strains arising from the interfacing of the magnetic layer to underlying and/or capping layers. The effect of strain on the structural properties of Ho thin films of different thickness has been studied by Bentall *et al* [6], who showed that above a critical thickness (115 Å) for Ho films on Y seed layers, dislocations reduced the misfit strain inherent in a pseudomorphically-grown structure. The helical magnetic structure of holmium provides a sensitive system for testing whether the magnetic behaviour, in terms of ordering temperature, helical pitch and critical exponent of the ordering, can be affected by a restricting sample dimension.

Previous studies on the magnetic behaviour of holmium films consist of the x-ray magnetic investigation that compared the temperature dependence of the plane helical phase in bulk holmium with that of a film of 20 000 Å thickness [7], a neutron scattering study on a film of 5000 Å thickness [8], and a neutron scattering investigation on films of thickness down to 50 Å [9]. In this work magnetic x-ray diffraction is used to compare the temperature dependence of the magnetic behaviour of the plane helical phase in films of 1000 monolayers (ML), 100 ML, and 50 ML. This study was carried out at the Ho $L_{III}$ resonant edge to benefit from the ∼50 times enhancement factor in magnetic scattering and using polarization analysis of the scattered beam to improve the ratio of the magnetically scattered signal over the charge scattered background.

## 2. Experimental and analytical methods

### *2.1. Sample fabrication and characterization*

The three samples used in this study were grown by molecular beam epitaxy (MBE) at the LaMBE facility at Oxford University following the growth method outlined in the work of Jehan *et al* [10]. The samples consist of a high-quality sapphire ($Al_2O_3$) ($11\bar{2}0$) substrate of size $12 \times 10 \times 1$ mm$^3$ onto which was deposited successively a niobium (110) buffer layer

of thickness 1100 Å and an (0001) yttrium seed layer of thickness 1350 Å. The holmium film was grown onto the yttrium seed layer with the [001] direction perpendicular to the surface of the sample. In the hcp structure the unit cell $c$ dimension corresponds to two atomic layer spacings. Thus the thicknesses of the Ho films are 2808 Å (1000 ML), 281 Å (100 ML) and 140 Å (50 ML). The epitaxial holmium film was capped with 100 Å of yttrium to prevent sample oxidation. Typical interfaces correspond to ±2 ML [10].

The rare earths were deposited at a rate of 0.5 Å $s^{-1}$ at a substrate temperature of 500 °C. Growth was monitored *in situ* and analysed in real-time using reflection high-energy electron diffraction (RHEED). Further characterization of the samples has been made using a high-resolution four-circle x-ray diffractometer. In these samples no attempt was made to match the lattice constants $a$ of the Y seed layer and the Ho film. The hexagonal cell dimension $a$ is 1.9% greater in Y than in Ho (at room temperature), resulting in an Ho film that is under tensile stress at the interfaces. However, the detailed measurements by Bentall *et al* [6] of strain as a function of Ho thickness in the Ho-on-Y system suggest that the mismatch strain should in fact be substantially relieved in all three samples. In order to determine directly the strain levels present in our samples, high resolution x-ray scans through Ho(002) at room temperature were carried out. These showed that the Ho $c$ parameter was only slightly less than the bulk value in each case (0.13%–0.39%). The mosaic spreads were also similar at 0.40°–0.45°, which are significantly larger than the reported value for bulk holmium [11]. It should be noted that strain due to lattice clamping of the epitaxial films by the substrate is not significant in our case because the relevant thermal expansion coefficients of the rare earth metals and sapphire are comparable. We conclude that elastic strain levels are low in all three samples, while the relief of mismatch strain has resulted in significant mosaic spread and also shortened the correlation length in the 1000 ML sample.

### *2.2. Experimental techniques*

The magnetic structure of these Ho films was studied by taking scans along the [00$L$] direction in reciprocal space, concentrating on the magnetic satellites that occur in association with the (002$n$) Bragg peaks from the crystal structure. The data were taken at the ESRF using the XMaS bending magnet beamline. In order to maximize the signal-to-noise ratio for these studies of extremely thin magnetic films, the incident photon energy was tuned to the Ho $L_{III}$ edge (8.073 keV), corresponding to the resonant E1 ($2p_{3/2} \rightarrow 5d$) transition [11]. This energy corresponds to the maximum of the Ho fluorescence signal, thus polarization analysis of the scattered beam was used to select the $\pi$ polarized magnetically scattered beam from the $\sigma$ polarized charge scattering. The polarization analyser has the further advantage of filtering out the fluorescence signal, a few 100 eV lower in energy.

A double mirror harmonic rejection system was used to remove the high energy harmonics, thus reducing some of the background. A monitor using a Bicron NaI(Tl) scintillation detector and a Mylar scattering foil allowed normalization of the data.

The samples were mounted in a closed-cycle cryostat with the [00$L$] direction initially perpendicular to the incident beam. The sample temperature was monitored via a thermocouple attached to the copper cryostat mount, temperature stability of the system was observed to be 0.01 K over several hours.

A graphite (006) polarization analyser crystal was used to optimize the signal-to-noise ratio of the coherent RXMS signal. The graphite (006) analyser crystal had a mosaic spread of 0.35° and a peak reflectivity of 13% at 7.828 keV. The polarization of the incident x-ray beam was chosen to be 99.2% within the $\sigma$ plane. Polarization analysis was used as a tool to cut the background and improve the signal-to-noise ratio.

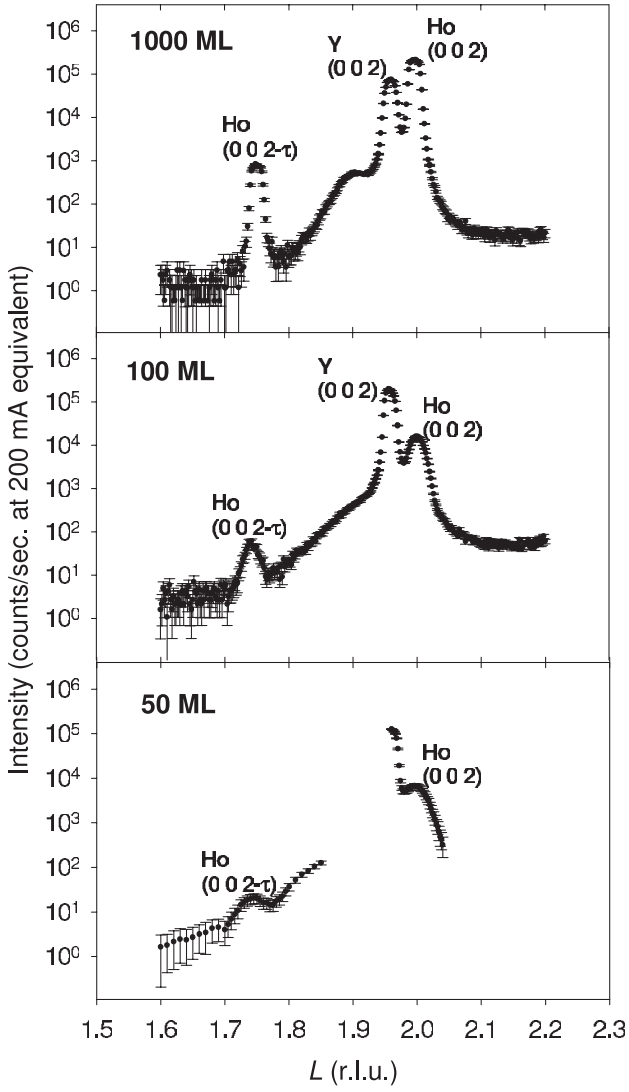


**Figure 2.** Specular [00$L$] scans of the RXMS scattering from the three samples at 80 K, illustrating the Ho(002) charge peak, Ho(002-$\tau$) magnetic peak and the Y(002) charge peak. The x-ray beam energy was 8.073 keV (Ho $L_{III}$ edge) and $\sigma \rightarrow \pi$ polarization analysis was used.

## 3. Results

Data on the magnetic structure along the $c$ axis was obtained by making [00$L$] scans over the Bragg charge peaks and magnetic satellites. Typical scans for the 1000, 100 and 50 ML samples at 80 K are shown in figure 2. The scans show, in order of increasing $L$, the Ho magnetic satellite (002-$\tau$), the Y seed layer charge peak (002) and the Ho charge peak (002). The broad peak around $L = 1.9$ was observed by Helgesen *et al* [7], who attributed it to interfacial features associated with the Y/Ho/Y structure. Comparing scans for the 1000 and 100 ML samples it is seen that both of the Ho peaks, the (002-$\tau$) magnetic satellite and the $L = 2$ charge peak, scale with Ho thickness, being ten times greater for the 1000 ML sample. The fact that this factor of 10 is substantially smaller than the factor of 100 that would

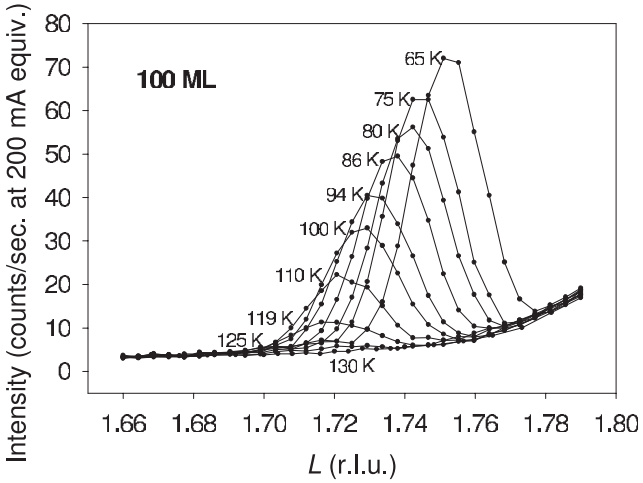


**Figure 3.** Growth of the Ho(002-$\tau$) magnetic peak on cooling the 100 ML sample.

be expected for coherent scattering indicates a greater degree of incoherence in the 1000 ML sample. This is expected as strains arising from interfacing with seed layer and cap are relieved by dislocations. The same effect is seen in the observation that the intensity of the 100 ML sample is twice the strength of the 50 ML sample rather than the expected factor of four. The intensities of the Y(002) charge peak are essentially equal when corrections for the absorption of the overlying Ho film are taken into account. Subsequent scans, taken over a temperature range 65–140 K, were confined to $L$ values spanning the Ho(002-$\tau$) magnetic scattering peak and the Ho ($L = 2$) charge peak.

The variation of the Ho(002-$\tau$) magnetic peak with temperature for the 100 ML sample is shown in figure 3. The magnetic peak lies on a sloping background which originates from the tail of the broad feature at $L = 1.9$ discussed above. The fit to the magnetic satellite peak determines values of $\tau$, linewidth and area corresponding to the periodicity of the helical magnetic structure, the magnetic correlation length and the number of aligned Ho moments respectively. The peaks have been fitted using two Gaussian functions: the first fits the Ho(002-$\tau$) magnetic peak and the second fits the tail of the broad feature. The use of the second Gaussian function was found to be the optimum method of fitting the unconventional sloping background.

### *3.1. Dependence of $\tau$ on thickness and temperature*

The size of the magnetic modulation wavevector $\tau$ is determined by calculating the difference in position of the (002-$\tau$) magnetic peak and the (002) charge peak at each temperature. The position of the magnetic satellite decreases in reciprocal space for all samples as the temperature increases to $T_N$, as shown in figure 3. The position of the charge peak increases linearly with increasing temperature. This shift means that in the Ho film the $c$ axis contracts as the temperature increases, as observed by Helgesen *et al* [7], who related this contraction to a magnetostrictive effect. It is observed that in this temperature interval the $a$ axis expands as the temperature increases with a linear coefficient of about one half of the observed $c$ axis coefficient [12], which leaves the volume of the unit cell approximately constant. Values of $\tau$ are corrected for the change of the lattice constant $c$ with temperature by scaling the Ho Bragg peak to $L = 2$ at each temperature and using this scaling to normalize the value of $\tau$.

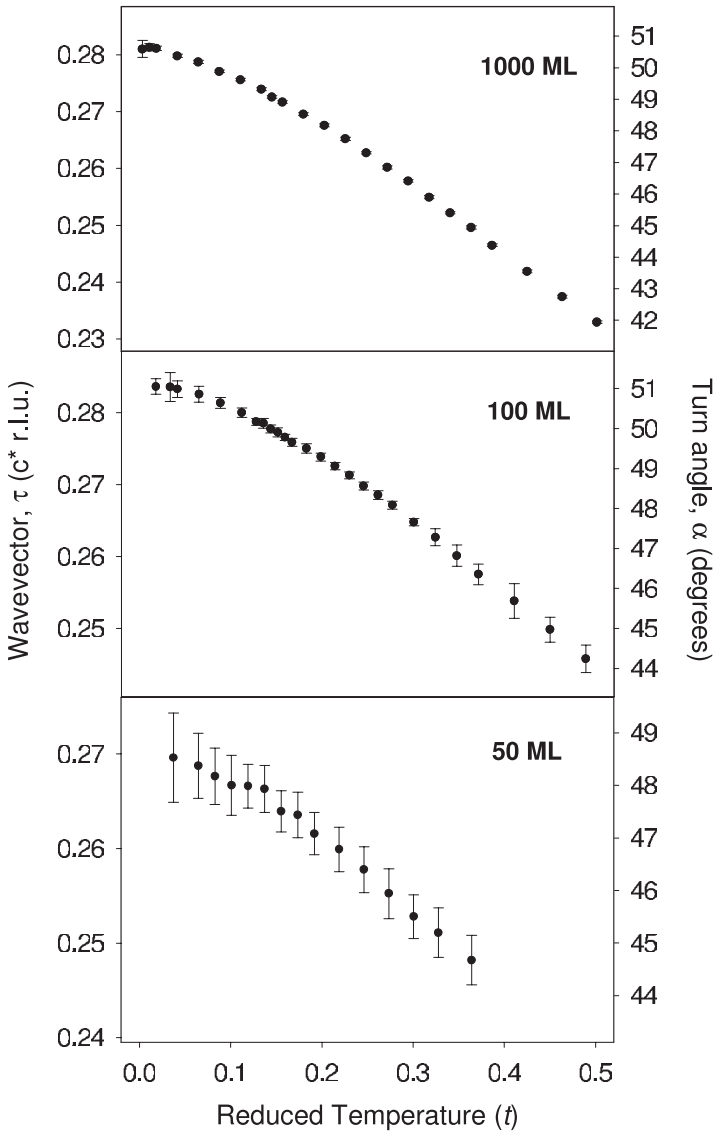


**Figure 4.** The helical modulation vector, $\tau$ ($c^*$ r.l.u.), plotted against reduced temperature for all three samples. Reduced temperature is defined as $t = (T_N - T)/T_N$.

These corrected values of $\tau$, plotted against reduced temperature $t$ where $t = (T_N - T)/T_N$, are shown in figure 4. The figure also shows the corresponding turn angle $\alpha$, from plane to plane, where $\alpha = 180\tau/\pi$ (in degrees). It is seen that, for the 50 ML sample near $T_N$, $\tau = 0.269c^*$, giving an angle $\alpha = 48.4°$. This equates to ≈6.6 Ho layers in a magnetic structural unit and thus the 50 ML sample contains only 7.6 complete helices of the magnetic structure near $T_N$.

The data in figure 4 show a similar trend of $\tau$ versus $t$ for all sample thicknesses. The gradient of the $\tau$ versus $t$ curve is similar in the 1000 and 100 ML films but is noticeably different for the 50 ML film. For all samples the gradient of the $\tau$ curve gets shallower near to

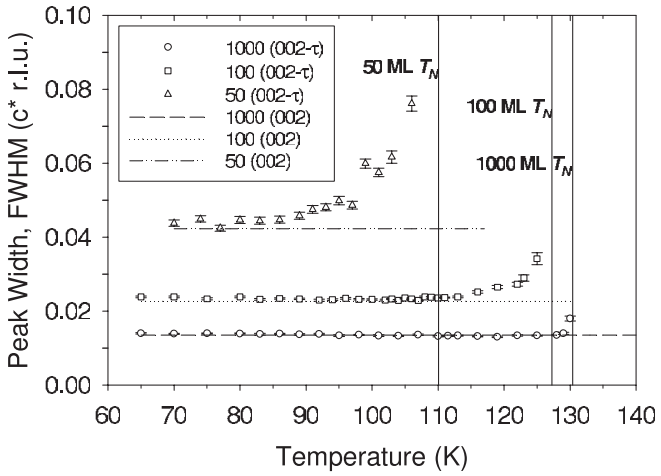


**Figure 5.** The temperature dependence of the widths of the Ho(002-$\tau$) magnetic satellite and Ho(002) charge peak, for the three films.

$T_N$. This is especially clear in the 50 ML sample, where the rate of change near $T_N$ indicates that $\alpha$ is reaching a maximum value.

### *3.2. Dependence of linewidth on thickness and temperature*

The temperature dependence of the widths of the Ho(002-$\tau$) magnetic satellite and Ho(002) charge peaks, for the three films, are shown in figure 5. The Ho(002) charge peak widths are shown in the figure as three solid horizontal lines. The (002) widths are seen to be temperature independent below $T_N$ for all three samples, and the linewidths are seen to increase as the Ho thickness decreases. The magnetic linewidths follow the same trend at temperatures such as 80 K. The linewidth of the Ho(002-$\tau$) magnetic peak is seen to increase as the sample temperature rises to $T_N$ for all film thicknesses, although it is more pronounced in the 50 ML film. In figure 5 the linewidths for the 50 and 100 ML samples are in agreement with the thicknesses of the films, but the linewidth for the 1000 ML sample is much too great to correspond to the 1000 ML thickness. The observation of an extremely thin peak for the sapphire substrate confirms that the instrumental resolution does not contribute appreciably to the 1000 ML linewidth. The observed linewidth for the sample corresponds to an effective coherent thickness of $\sim$400 Å arising from structural imperfections which relieve the strain in the film.

The linewidth of the magnetic satellite is determined by the magnetic coherence length along the *c* axis. In figure 5 the peak widths at $<$80 K are consistent with magnetic coherence lengths determined by the effective coherent thickness ($\sim$400 Å) set by structural imperfections in the 1000 ML (2800 Å) Ho film and by the film thicknesses of the 100 ML (280 Å) and 50 ML (140 Å) Ho films, respectively. As the temperature approaches $T_N$ in each case the coherence length decreases, causing the linewidths to increase as $T \rightarrow T_N$.

### *3.3. Dependence of integrated intensity on thickness and temperature*

The integrated intensities of the fitted Ho(002-$\tau$) magnetic peak at each temperature in all three films are shown in figure 6. In the left panels the intensities are plotted against temperature

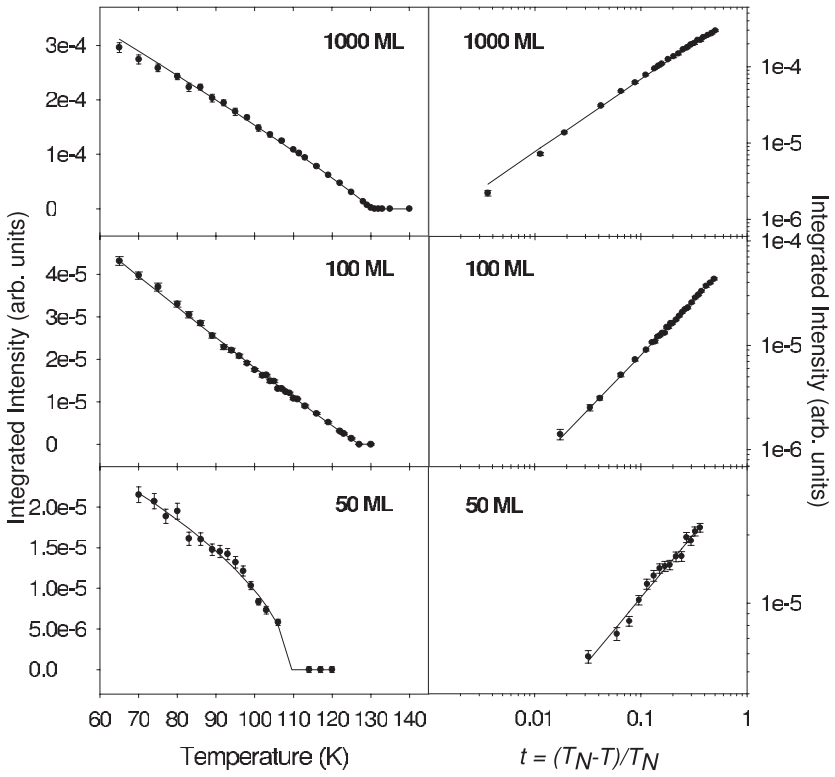


**Figure 6.** Left panels: power law fits to the graphs of integrated intensity versus temperature for the (002-$\tau$) satellite for all three samples. The power law is defined as $I \propto (1 - T/T_N)^{2\beta}$ and the fits shown are over all data points below $T_N$. Right panels: straight line fits of the integrated intensities against reduced temperature ($t$). The gradient of the fitted line is equal to $2\beta$ and the fits are conducted over all data points below $T_N$. Note the different $y$ axis scales.

**Table 1.** Values of $T_N$, $\beta$, $\tau$ (near $T_N$) and FWHM of the Ho(002) charge peak for the three holmium films.

| Sample (ML) | $T_N$ (K) | $\beta$ | $\tau$ ($c^*$ r.l.u.) near $T_N$ | FWHM ($c^*$ r.l.u.) of Ho(002) |
|---|---|---|---|---|
| 1000 | $130.41 \pm 0.07$ | $0.49 \pm 0.05$ | $0.281 \pm 0.001$ | $0.0136 \pm 0.0001$ |
| 100 | $127.27 \pm 0.07$ | $0.52 \pm 0.04$ | $0.284 \pm 0.001$ | $0.0227 \pm 0.0002$ |
| 50 | $110 \pm 1$ | $0.28 \pm 0.05$ | $0.269 \pm 0.003$ | $0.0422 \pm 0.0004$ |

and are fitted to a power law, while in the right panels the same intensities are plotted against reduced temperature and are fitted to a straight line. The fitted power law expression is of the form $I \propto (1 - T/T_N)^{2\beta}$, where $I$ is the integrated intensity and $\beta$ is the critical ordering exponent. The straight line is of the form $\ln I = 2\beta \ln t + \ln k$, where $k$ is a constant and $t$ is the reduced temperature, defined as $t = (T_N - T)/T_N$. The power law fit is used for determining $T_N$, while the straight line fit is used for calculating the critical ordering exponent $\beta$. The fits shown in figure 6 give rise to values of $T_N$ and $\beta$ that are summarized in table 1 with the values of $\tau$ and the linewidths for each film. It is seen that $T_N$ decreases with reducing film thickness, and the decrease is more pronounced in the 50 ML film. The value of the critical exponent $\beta$ is similar for the 1000 ML and the 100 ML films, but is significantly less in the 50 ML film.

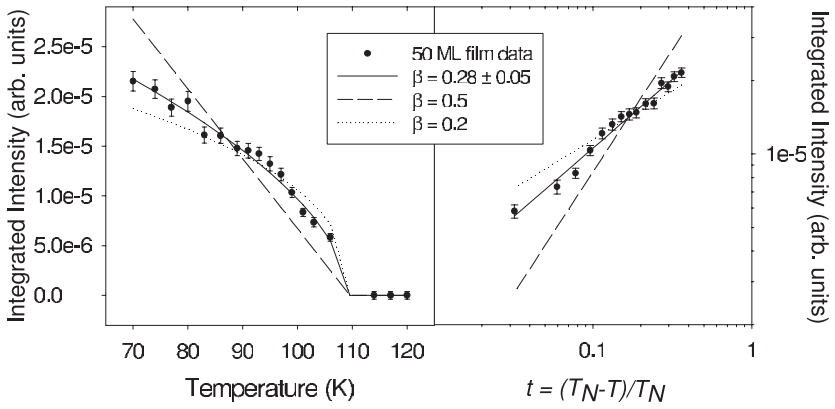


**Figure 7.** Integrated intensity against temperature (left panel) and reduced temperature (right panel) for the 50 ML film. The solid lines are the fits shown in figure 6. The dashed and dotted lines are fits performed with fixed $\beta$ values of 0.5 and 0.2 respectively. $T_N$ is fixed as 110 K for the power law fits.

The determination of values for $T_N$ and $\beta$ for the 50 ML film data is hindered by the limited number of data points close to $T_N$. In figure 7 the effect of different possible values of $\beta$ in fitting the data are shown. It is seen that using values of critical exponent $\beta = 0.5$ and 0.2 result in fits which are evidently poorer than for $\beta = 0.28$—but by means of such fits the error on the best value of $\beta$ can be assessed as $\beta = 0.28 \pm 0.05$. It is thus established that the critical exponent for the 1000 ML and the 100 ML films are well described with $\beta = 0.50$ but that for the 50 ML film $\beta$ is substantially lower.

## 4. Discussion

The aim of this study has been to investigate the effect on the magnetism of the Ho helical phase (20–132 K in bulk Ho) of reducing the sample dimension along the helical $c$ axis. The range of thickness variation of the samples used is 1000–50 ML and the temperature range of the investigation was from 65 to 130 K. Characterization by laboratory x-ray diffraction analysis showed that the mismatch strain had been substantially relaxed even in the 50 ML sample, and the three samples were of similar structural quality.

The magnetic features that may be affected by limiting the sample extent along the $c$ axis are the structural parameter $\tau$ (related to the helical turn angle $\alpha = \tau * 180/\pi$) and the parameters mediating the transition to the paramagnetic state, the Néel temperature $T_N$ and the critical exponent $\beta$.

In figure 4 it is seen that the value of $\tau$ at $T_N$ is greater in the 1000 and 100 ML samples than in the 50 ML sample. However, in terms of actual temperature, where for the 50 ML sample $T_N = 110$ K whereas for the 100 and 1000 ML samples $T_N \approx 130$ K, the value of $\tau$ is seen to depend on temperature but there is no evidence for dependence on sample thickness in the range 1000–50 ML.

The transition between the ordered helical phase and the paramagnetic phase is characterized by the Néel temperature $T_N$ and the critical exponent $\beta$. In table 1 it is seen that there is a small decrease in $T_N$ from the 1000 ML to the 100 ML (130.4–127.3 K) but a much larger decrease (to 110 K) to the 50 ML sample. Similarly the critical exponent values for the 1000 and 100 ML are the same within errors at $\beta \approx 0.5$, while that for the 50 ML sample is much smaller at $\beta = 0.28 \pm 0.05$.

The value of the critical exponent measured for the transition in bulk Ho, $\beta = 0.39 \pm 0.04$ [7], is substantially smaller than those for the 1000 and 100 ML samples. In an experiment on a thin film with strain-free interfaces a value of $\beta = 0.37 \pm 0.05$ was measured [8], which agrees with the bulk value. However, in another study on which a 1000 Å film was contained between Y layers a value of $\beta = 0.5$ was measured [9], which agrees with the present work. The precision measurements of the $c$ parameter made in our work indicate that this observed difference in $\beta$ from the bulk value cannot be attributed to simple strain but may be associated with the crystalline defects in the films that arise to relieve the strain.

In figure 6 the temperature evolution of the scattering intensity with increasing temperature as $T \rightarrow T_N$ is seen to be quite different for the 50 ML sample from the 1000 and 100 ML samples. Analysis of this evolution, illustrated in figure 7, gives a value for the 50 ML sample of $\beta = 0.28 \pm 0.05$. As this sample is of similar structural condition to the 1000 and 100 ML samples, some other effect reduces $\beta$ to this value. It is attractive to propose that the limiting of the magnetic correlation along the $c$ axis, limited to 50 ML by sample construction but further reduced by the decrease in magnetic correlation length as $T \rightarrow T_N$ (as observed in figure 5), reduces the dimensionality of ordering to quasi-two-dimensional, which is reflected in this value of the critical exponent.

## Acknowledgments

This work was funded by the UK Engineering and Physical Sciences Research Council (EPSRC). The measurements were conducted on the EPSRC-funded XMaS beamline at the ESRF and we are grateful to the beamline team for their help and expertise. ADFH acknowledges the receipt of an EPSRC research studentship.

## References

[1] Wyckoff R W 1966 *Crystal Structures* (New York: Interscience)
[2] Koehler W C, Cable J W, Wilkinson M K and Wollan E O 1966 *Phys. Rev.* **151** 414
[3] Felcher G P, Lander G H, Arai T, Sinha S K and Spedding F H 1976 *Phys. Rev.* B **13** 3034
[4] Pechan M J and Stassis C 1984 *J. Appl. Phys.* **55** 1900
[5] Cowley R A and Bates S 1988 *J. Phys. C: Solid State Phys.* **21** 4113
[6] Bentall M J, Cowley R A, Ward R C C, Wells M R and Stunault A 2003 *J. Phys.: Condens. Matter* **15** 7155
[7] Helgesen G, Hill J P, Thurston T R, Gibbs D, Kwo J and Hong M 1994 *Phys. Rev.* B **50** 2990
[8] Cowley R A, Gehring P M, Gibbs D, Goff J P, Lake B, Majkrzak C F, Vigliante A, Ward R C C and Wells M R 1998 *J. Phys.: Condens. Matter* **10** 6803
[9] Leiner V, Labergerie D, Siebrecht R, Sutter C and Zabel H 2000 *Physica* B **283** 167
[10] Jehan D A, McMorrow D F, Cowley R A, Ward R C C, Wells M R, Hagmann N and Clausen K N 1993 *Phys. Rev.* B **48** 5594
[11] Gibbs D, Grübel G, Harshman D R, Isaacs E D, McWhan D B, Mills D and Vettier C 1991 *Phys. Rev.* B **43** 5663
[12] Steinitz M O, Kahrizi M and Tindall D A 1987 *Phys. Rev.* B **36** 783